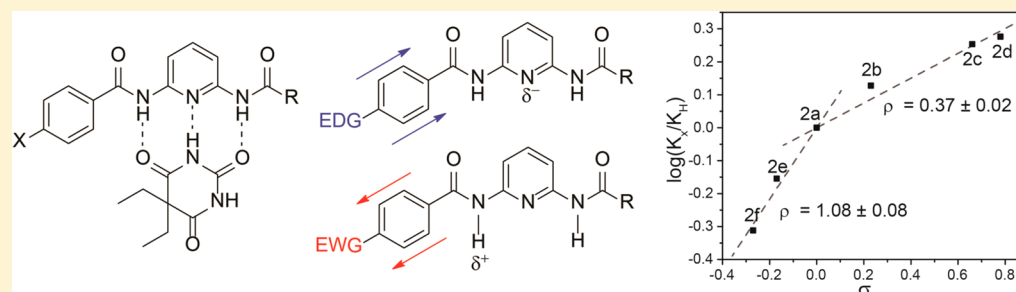


Linear Free Energy Relationships Reveal Structural Changes in Hydrogen-Bonded Host–Guest Interactions

Jacqueline M. McGrath and Michael D. Pluth*

Department of Chemistry and Biochemistry, Materials Science Institute, University of Oregon, Eugene, Oregon 97403-1253, United States

S Supporting Information



ABSTRACT: Hydrogen bond strength in host–guest systems is modulated by many factors including preorganization, steric effects, and electronic effects. To investigate how electronic effects impact barbiturate binding in bifurcated Hamilton receptors, a library of receptors with differing electronic substituents was synthesized and ^1H NMR titrations were performed with diethyl barbital. The Hammett plot revealed a clear break between the different electronic substituents suggesting a change in binding conformation. The titration data were complimented with computational studies confirming the change in structure.

Host–guest binding plays a key role in many types of chemistry, ranging from molecular recognition to catalysis.^{1–6} Understanding how structural changes influence such interactions enables control over guest binding and facilitates the molecular design of synthetic supramolecular complexes. Various factors, including steric and electronic effects as well as host–guest preorganization, can all affect host–guest complex stability and guest exchange rates.^{5,7,8} To better understand the interplay of these forces in hydrogen-bonded systems, we recently investigated barbiturate binding to 2,6-diamidopyridines, a bifurcated form of macrocyclic Hamilton receptors to determine the differential effects of steric interactions and host preorganization on guest binding affinities.⁹ Toward understanding the impacts of electronic substitution on guest binding in hydrogen-bonded systems, we report here binding studies on 2,6-diaminopyridines with barbital that reveal changes in host–guest structure as a function of electronic substitution.

Because 2,6-diamidopyridines bind barbiturates through complementary hydrogen bonding, we chose to use a system in which one of the amides contained a phenyl substituent with an electron withdrawing or donating group in the *para* position. This design allowed for electronic changes in the phenyl substituent to modulate the acidity of the amide N–H as well as the basicity of the pyridine nitrogen (Figure 1).^{10,11} Inclusion of electron withdrawing groups should acidify the amide, making it a better hydrogen bond donor, whereas electron donating groups should not only decrease the amide acidity but also increase the electron density of the pyridine nitrogen,

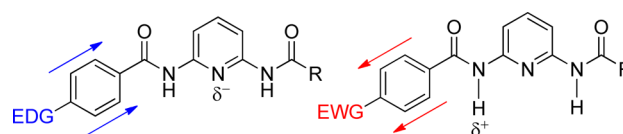


Figure 1. Effects of electron donating and withdrawing on the electron density of the 2,6-diamidopyridine receptors.

making it a better hydrogen bond acceptor. Although these two effects are opposing, the acidification of the amide NH is expected to be a larger effect due to the closer proximity to the substituted phenyl group.

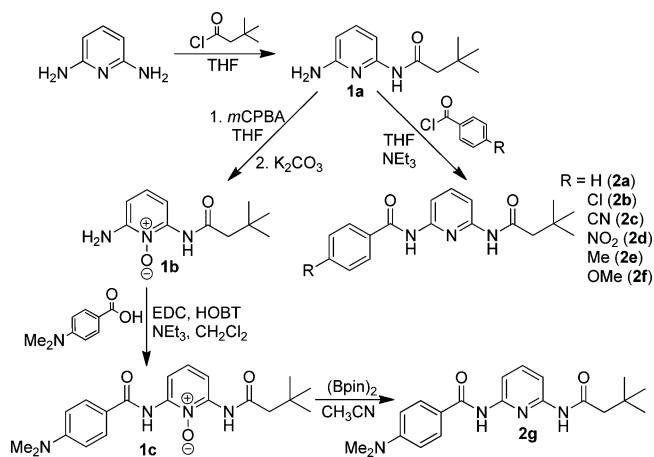
To prepare the desired compounds, precursor **1a** was prepared by coupling 3,3-dimethylbutyryl chloride with 2,6-diaminopyridine using excess diaminopyridine as the base in THF. Compounds **2a–f** were prepared by treatment of the corresponding acid chlorides with **1a** (Scheme 1). To prepare the *p*-dimethylamino substituted compound, the pyridine nitrogen of **1a** was first oxidized with *m*CPBA to afford **1b**, which was then coupled to *p*-dimethylamino benzoic acid using EDC and HOBT.¹² The resultant *N*-oxide product (**1c**) was then reduced with (Bpin)₂ to afford **2g**.¹³

To measure the binding affinity of the differently substituted **2a–g** with diethyl barbital, ^1H NMR titrations were performed for each host–guest system in CDCl₃. Because the binding involves hydrogen bonding between the receptor and barbital,

Received: October 10, 2014

Published: November 14, 2014

Scheme 1. Synthesis of 2,6-Diamidopyridines 2a–g



the N–H ^1H NMR resonances of the amides on both the host and the guest change during the course of the titration (Figure 2). Using the tabulated chemical shift data of the barbital N–H,

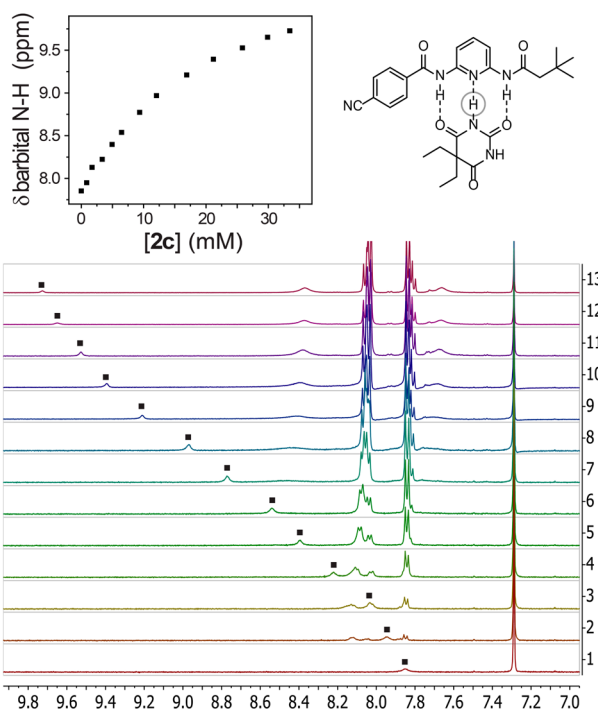


Figure 2. Representative ^1H NMR (500 MHz, 25 °C, CDCl_3) titration of diethyl barbital with **2c**. The stacked ^1H NMR titration spectra and tabulated plot of the N–H chemical shift data from the ^1H NMR titration are shown.

the resultant binding isotherms were fit to a 1:1 model, based on previous studies investigating the binding stoichiometry of compounds such as **2a–g** with diethyl barbital.⁹ All measurements were repeated at least in triplicate to ensure reproducibility of the binding affinities.

Measurement of the binding constants of **2a–g** with diethyl barbital revealed that electron withdrawing groups result in the highest binding affinity, whereas electron donating groups weakened guest binding. Binding affinities for **2g**, which contained the most electron donating group, were too low to measure reproducibly. These results suggest that acidification of the amide N–H plays a larger role in guest binding than

increasing the basicity of the pyridine nitrogen, which is consistent with the closer proximity of the amide group to the electronically substituted phenyl group. To quantitatively compare the impacts of electronic effects on barbital binding, we used the experimentally determined binding affinities to construct a Hammett plot using the corresponding σ_p values for each substituent (Figure 3).^{14,15} The resultant

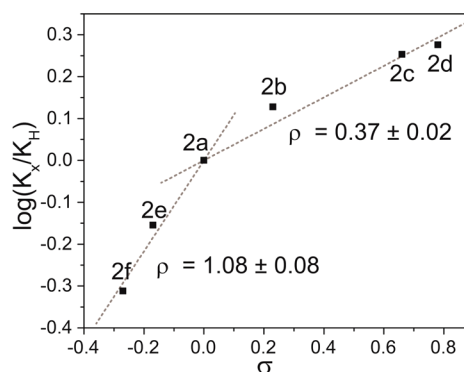


Figure 3. Hammett plot of hosts **2a–f** binding diethyl barbital. Binding constants were obtained by following the barbital N–H resonance using ^1H NMR spectroscopy (500 MHz, 25 °C, CDCl_3).

Hammett plot has a positive slope, which confirms that negative charge buildup is stabilized during the guest binding process, an effect that is consistent with both increased amide acidity and increased electron density on the pyridine nitrogen.^{16,17} The slope of the Hammett plot, however, shows a clear break between the electron donating and withdrawing groups, with ρ values of 1.08 ± 0.08 and 0.37 ± 0.02 , respectively.¹⁸ This bimodal (or curved) Hammett plot suggests a change in binding conformation between the hosts with electron withdrawing and donating groups, respectively.^{19–21} Such a change could be due to the shorter hydrogen bonds formed between the host and guest upon acidification of the amides with inclusion of electron withdrawing groups.^{10,11,22–25}

To further investigate this nonlinear Hammett plot, we used computational studies to determine whether the break in the Hammett plot was related to changes in host–guest structure. Structures for **2a–f** coordinated to diethyl barbital were optimized at the B3LYP/6-31+G(d,p) level of theory and the IEF-PCM solvation model for CHCl_3 , which has been shown to correlate well with experimental binding affinities in similar systems.⁹ Calculations using dispersion-corrected functionals were also performed and provided similar results. For each optimized geometry, the NH–O(barbital) and N–HN–(barbital) hydrogen bond lengths were measured and compared to that of **2a** ligated to barbital (Figure 4). As expected, the distal N–H of the alkyl amide did not change upon electronic substitution to the phenyl ring because the alkyl N–H is too far away from the electronic modulation to expect a significant contribution. By contrast, the amide N–H proximal to the benzene ring changes linearly with electronic substitution. Similarly, the hydrogen bond to the pyridyl nitrogen changes, although not linearly, with electronic substitution. Taken together, the structural difference upon electronic substitution are consistent with a change in equilibrium geometry, which would correspond to a bimodal (or curved) Hammett plot, and is consistent with the observed experimental results.

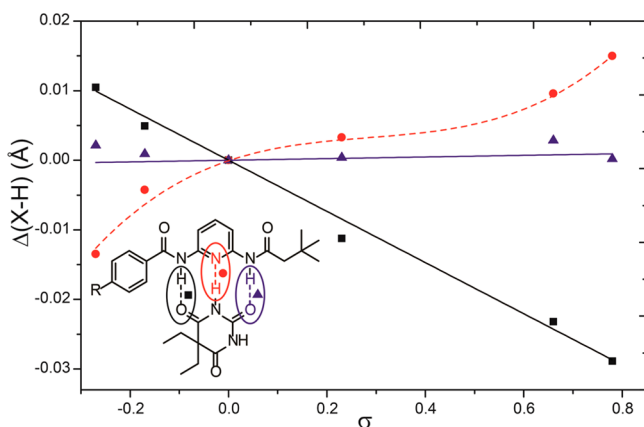


Figure 4. Comparison of the NH–O(barbital) and N–HN(barbital) hydrogen bonding distances for **2a–f** hydrogen bonded to diethylbarbital. Calculations were performed in Gaussian using the B3LYP/6-31+G(d,p) level of theory and the IEF-PCM solvation model for CHCl₃.

In conclusion, we have shown that binding of barbiturates to 2,6-diaminopyridines with different electronic structures produces a nonlinear Hammett plot, which is characteristic of changes in host–guest structure upon modulation of electronic structure. These results were supported both experimentally, using determined binding affinities, and computationally, using structural comparisons of optimized host–guest geometries. Taken together, these studies highlight how changes in electronic structure in hydrogen bonding assemblies can result not only in changes in binding affinities but also in changes in the assembled structure, thus providing insight into the factors controlling structural changes in the hydrogen-bonded complexes between the receptors and barbiturate guest.

EXPERIMENTAL SECTION

Materials and Methods. All commercially available reagents were used as received. Deuterated solvents were used as received. Anhydrous solvents used for syntheses were collected from a solvent purification system. Reactions were monitored by TLC on Silicagel 60 F₂₅₄ plates, and the products were purified on an automated chromatography instrument using SiliaFlash F60 SiO₂. NMR spectra were recorded at the indicated frequencies on either a 300 or 500 MHz spectrometer. Chemical shifts are reported in parts per million (δ) and are referenced to residual protic solvent resonances. The following abbreviations are used in describing NMR couplings: (s) singlet, (d) doublet, (t) triplet, (m) multiplet, and (b) broad; coupling constants are reported in hertz (Hz).

General Procedure Binding Constant Determination. Binding studies were performed in CDCl₃ for host molecules **2a–g** and were monitored by ¹H NMR spectroscopy. In a typical CDCl₃ titration, 2.00 mL of 1.0 mM barbital was prepared. The guest solution was then divided such that 1.00 mL was placed into an NMR tube and the other 1.00 mL was used to create a second solution containing 50–75 mM host. An initial spectrum of the guest was recorded, after which aliquots (5–100 μ L) of the host solution were added until the N–H resonance of barbital no longer shifted. The resultant curves were fit using a 1:1 model, and the K_{assoc} was obtained.²⁶

Computational Details. Calculations were performed using the Gaussian 09²⁷ software package using the GaussView²⁸ 5.0 graphical user interface. Geometry optimizations and unscaled frequency calculations were performed at the B3LYP/6-31+G(d,p) level of theory using the IEF-PCM solvation model for chloroform. Frequency calculations were performed on all converged structures confirming that they corresponded to local minima. In all cases, the lowest energy

conformer was used to compare the relative energetics of the calculated species.

Syntheses. *N*-(6-Aminopyridin-2-yl)-3,3-dimethylbutanamide (**1a**). A round-bottom flask was charged with dry THF (100 mL) and 2,6-diaminopyridine (1.04 g, 9.5 mmol). The flask was then lowered into an ice bath and deoxygenated by sparging with N₂. 3,3-Dimethylbutyryl chloride (0.60 mL, 4.3 mmol) was added to an addition funnel containing dry THF (25 mL), and the resultant solution was then added slowly to the diaminopyridine solution over the course of 1 h while stirring at 0 °C under N₂. Once the addition of the acid chloride was complete, the ice bath was removed and the reaction was allowed to warm to room temperature overnight while stirring under N₂. The precipitate from the reaction was filtered, and the resultant filtrate was concentrated by rotary evaporation. The crude product was purified by column chromatography (SiO₂, EtOAc) to afford a solid (0.61 g, 69%). Mp = 113–114 °C. ¹H NMR (300 MHz, CDCl₃) δ : 7.77 (s, 1H), 7.59 (d, *J* = 8.0, 1H), 7.48 (t, *J* = 8.0, 1H), 6.28 (d, *J* = 7.5, 1H), 4.43 (s, 2H), 2.24 (s, 2H), 1.11 (s, 9H). ¹³C{¹H} NMR (125 MHz, CDCl₃) δ : 170.3, 156.7, 149.4, 140.5, 104.2, 103.2, 51.7, 31.3, 29.9. HRMS (ESI-TOF) *m/z*: [M]⁺ calcd for [C₁₁H₁₇N₃O₂Na]⁺, 230.1269; found 230.1275.

2-Amino-6-(3,3-dimethylbutanamido)pyridine 1-Oxide (1b). **1a** (0.20 g, 0.97 mmol) was added to a round-bottom flask containing THF (75 mL). *m*CPBA (0.22, 1.3 mmol) was then added to the flask, and the reaction was allowed to stir overnight at room temperature. The reaction mixture was concentrated, and the residue was taken up in EtOAc and washed 3 \times with 75 mL of saturated K₂CO₃. The organic layer was concentrated using a rotary evaporator to yield the product as a yellow solid (0.18 g, 84%). Mp = 119–120 °C. ¹H NMR (500 MHz, CDCl₃) δ : 9.95 (s, 1H), 7.78 (d, *J* = 8.5, 1H), 7.19 (t, *J* = 8.5, 1H), 6.48 (d, *J* = 8.0, 1H), 5.77 (s, 2H), 2.40 (s, 2H), 1.12 (s, 9H). ¹³C{¹H} NMR (125 MHz, CDCl₃) δ : 170.7, 148.6, 142.5, 130.1, 102.7, 102.1, 51.6, 31.3, 29.8. HRMS (ESI-TOF) *m/z*: [M]⁺ calcd for [C₁₁H₁₈N₃O₂]⁺, 224.1399; found 224.1401.

2-(4-(Dimethylamino)benzamido)-6-(3,3-dimethylbutanamido)pyridine 1-Oxide (1c). 4-Dimethylaminobenzoic acid (80 mg, 0.50 mmol) was added to a vial containing HOBT (70 mg, 0.55 mmol), EDC (0.11 g, 0.55 mmol), NEt₃ (80 μ L, 0.59 mmol), and CH₃CN (15 mL). The reaction mixture was allowed to stir for 1 h at 50 °C before addition of **1b** (0.10 g, 0.46 mmol). The reaction mixture was stirred overnight at 50 °C, after which the solvent was removed under vacuum. The crude product was purified by column chromatography (SiO₂, 1:1 EtOAc/hexanes) to afford the product as an off-white solid (80 mg, 49%). Mp = 158–159 °C. ¹H NMR (500 MHz, CDCl₃) δ : 10.63 (s, 1H), 9.85 (s, 1H), 8.31 (d, *J* = 8.5, 1H), 8.15 (d, *J* = 8.3, 1H), 7.94 (d, *J* = 8.5, 2H), 7.42 (t, *J* = 9.0, 1H), 6.82 (d, *J* = 8.5, 2H), 3.11 (s, 6H), 2.42 (s, 2H), 1.16 (s, 9H). ¹³C{¹H} NMR (125 MHz, CDCl₃) δ : 170.2, 164.9, 162.9, 149.8, 149.4, 140.9, 129.1, 126.3, 114.1, 109.6, 109.4, 55.5, 51.9, 31.4, 29.8. HRMS (ESI-TOF) *m/z*: [M + H]⁺ calcd for [C₂₀H₂₇N₄O₃]⁺, 371.2079; found 371.2083.

N-(6-(3,3-Dimethylbutanamido)pyridin-2-yl)benzamide (**2a**). A round-bottom flask was charged with dry THF (30 mL), **1a** (114.5 mg, 0.55 mmol), and NEt₃ (0.12 mL, 0.83 mmol). The flask was then lowered into an ice bath and deoxygenated by sparging with N₂. Benzoyl chloride (70 μ L, 0.61 mmol) was added to an addition funnel containing dry THF (10 mL), and the resultant acid chloride solution was then slowly added to the diaminopyridine solution while stirring in the ice bath under N₂. Once the addition of the acid chloride was complete, the ice bath was removed and the reaction was allowed to warm to room temperature overnight while stirring under N₂. The reaction was concentrated by rotary evaporation, and the crude product was taken up in EtOAc and washed 3 \times with 1 M NaOH. The organic layer was kept and concentrated under vacuum to afford the product as a white solid (0.15 g, 87%). Mp = 140–141 °C. ¹H NMR (500 MHz, CDCl₃) δ : 8.34 (s, 1H), 8.08 (d, *J* = 8.0, 1H), 7.99 (d, *J* = 8.0, 1H), 7.90 (d, *J* = 7.5, 2H), 7.78–7.73 (m, 2H), 7.58 (t, *J* = 7.5, 1H), 7.51 (d, *J* = 8.0, 2H), 2.26 (s, 2H), 1.12 (s, 9H). ¹³C{¹H} NMR (125 MHz, CDCl₃) δ : 170.3, 165.4, 149.6, 140.9, 134.2, 132.3, 128.9, 127.1, 109.7, 109.6, 51.8, 31.4, 29.8. HRMS (ESI-TOF) *m/z*: [M]⁺ calcd for [C₁₈H₂₁N₃O₂Na]⁺, 334.1531; found 334.1532.

4-Chloro-N-(6-(3,3-dimethylbutanamido)pyridin-2-yl)benzamide (2b). Disubstituted diaminopyridine **2b** was prepared according to the general procedure outlined for **2a** with the following quantities: 4-chlorobenzoyl chloride (50 μ L, 0.37 mmol) in THF (10 mL) was added slowly to **1a** (58.2 mg, 0.281 mmol) and triethylamine (0.10 mL, 0.70 mmol) in THF (30 mL). The solvent was removed, and the residue purified by column chromatography (SiO₂, 4:1 hexanes/EtOAc) to afford a white crystalline solid (95 mg, 97%). Mp = 149–151 °C. ¹H NMR (500 MHz, DMSO) δ : 10.49 (s, 1H), 10.07 (s, 1H), 8.01 (d, *J* = 8.5, 2H), 7.88 (d, *J* = 7.0, 1H), 7.81 (t, *J* = 7.5, 1H), 7.75 (d, *J* = 7.0, 1H), 7.60 (d, *J* = 8.5, 2H), 3.35 (s, 2H), 1.03 (s, 9H). ¹³C{¹H} NMR (125 MHz, DMSO) δ : 171.4, 165.3, 151.0, 150.5, 140.4, 137.2, 133.4, 130.3, 128.9, 111.3, 110.3, 49.5, 31.4, 30.1. HRMS (ESI-TOF) *m/z*: [M]⁺ calcd for [C₁₈H₂₁N₃O₂Cl]⁺, 346.1311; found 346.1322.

4-Cyano-N-(6-(3,3-Dimethylbutanamido)pyridin-2-yl)benzamide (2c). Disubstituted diaminopyridine **2c** was prepared according to the general procedure outlined for **2a** with the following quantities: 4-cyanobenzoyl chloride (228 mg, 1.38 mmol) in THF (10 mL) was added slowly to **1a** (238 mg, 1.15 mmol) and triethylamine (0.32 mL, 2.29 mmol) in THF (40 mL). The solvent was removed, and the residue was purified by column chromatography (SiO₂, 1:1 EtOAc/hexanes) to afford a white crystalline solid (0.31 g, 80%). Mp = 202–203 °C. ¹H NMR (500 MHz, CDCl₃) δ : 8.27 (s, 1H), 8.07–8.02 (m, 4H), 7.85–7.79 (m, 3H), 7.55 (s, 1H), 2.28 (s, 2H), 1.13 (s, 9H). ¹³C{¹H} NMR (125 MHz, CDCl₃) δ : 170.3, 163.6, 149.6, 148.9, 141.2, 138.1, 132.7, 127.8, 117.8, 115.9, 110.3, 109.7, 51.8, 31.4, 29.8. HRMS (ESI-TOF) *m/z*: [M]⁺ calcd for [C₁₉H₂₀N₄O₂Na]⁺, 359.1484; found 359.1499.

N-(6-(3,3-Dimethylbutanamido)pyridin-2-yl)-4-nitrobenzamide (2d). The disubstituted diaminopyridine **2d** was prepared according to the general procedure outlined for **2a** with the following quantities: 4-nitrobenzoic acid was stirred in thionyl chloride (3 mL) overnight at 65 °C. The thionyl chloride was removed, and the residue was taken up in THF (10 mL) and was then added slowly to **1a** (126.6 mg, 0.61 mmol) and NEt₃ (0.17 mL, 1.22 mmol) in THF (30 mL). The solvent was removed, and the residue was purified by column chromatography (SiO₂, 1:1 EtOAc/hexanes) to afford a white crystalline solid (0.20 g, 84%). Mp = 162–163 °C. ¹H NMR (500 MHz, CDCl₃) δ : 8.38 (d, *J* = 9.0, 2H), 8.10 (d, *J* = 8.5, 2H), 8.07–8.02 (m, 2H), 7.81 (t, *J* = 8.0, 1H), 7.61 (s, 2H), 2.29 (s, 2H), 1.14 (s, 9H). ¹³C{¹H} NMR (125 MHz, CDCl₃) δ : 170.4, 163.5, 150.0, 149.6, 148.9, 141.2, 139.6, 128.4, 124.1, 110.3, 109.7, 51.8, 31.4, 29.8. HRMS (ESI-TOF) *m/z*: [M]⁺ calcd for [C₂₀H₂₇N₄O₂]⁺, 355.2134; found 355.2123.

N-(6-(3,3-Dimethylbutanamido)pyridin-2-yl)-4-methylbenzamide (2e). Disubstituted diaminopyridine **2e** was prepared according to the general procedure outlined for **2a** with the following quantities: *p*-toluic acid was stirred in thionyl chloride (3 mL) overnight at 65 °C. The thionyl chloride was then removed under vacuum, and the residue taken up in THF (10 mL) and was then added slowly to **1a** (160.1 mg, 0.77 mmol) and triethylamine (0.22 mL, 1.54 mmol) in THF (30 mL). The solvent was removed, and the residue was purified by column chromatography (SiO₂, 1:1 EtOAc/hexanes) to afford a white crystalline solid (0.22 g, 81%). Mp = 159–161 °C. ¹H NMR (500 MHz, CDCl₃) δ : 8.28 (s, 1H), 8.09 (d, *J* = 8.5, 1H), 7.98 (d, *J* = 7.5, 1H), 7.83 (d, *J* = 8.0, 2H), 7.78 (t, *J* = 8.0, 1H), 7.60 (s, 1H), 7.32 (d, *J* = 8.0, 2H), 2.46 (s, 3H), 2.28 (s, 2H), 1.14 (s, 9H). ¹³C{¹H} NMR (125 MHz, CDCl₃) δ : 170.3, 165.5, 149.6, 149.3, 143.0, 141.1, 131.3, 129.6, 127.1, 109.6, 109.5, 51.8, 31.4, 29.8, 21.6. HRMS (ESI-TOF) *m/z*: [M]⁺ calcd for [C₁₉H₂₄N₃O₂]⁺, 326.1869; found 326.1877.

N-(6-(3,3-Dimethylbutanamido)pyridin-2-yl)-4-methoxybenzamide (2f). Disubstituted diaminopyridine **2f** was prepared according to the general procedure outlined for **2a** with the following quantities: *p*-anisic acid (73.9 mg, 0.489 mmol) was stirred in thionyl chloride (3 mL) at 65 °C overnight. The thionyl chloride was removed under vacuum, and the resulting residue taken up in THF (10 mL) was added slowly to **1a** (91.5 mg, 0.442 mmol) and triethylamine (0.12 mL, 0.882 mmol) in THF (30 mL). After solvent removal, the residue was purified by column chromatography (SiO₂, 1:1 EtOAc/hexanes) to afford a white crystalline solid (0.18 g, 95%). Mp = 171–

172 °C. ¹H NMR (500 MHz, CDCl₃) δ : 8.36 (s, 1H), 8.11 (d, *J* = 8.5, 1H), 7.98 (d, *J* = 8.0, 1H), 7.98 (d, *J* = 8.5, 2H), 7.82 (t, *J* = 7.5, 1H), 7.64 (s, 1H), 7.02 (d, *J* = 9.0, 2H), 3.92 (s, 3H), 2.28 (s, 2H), 1.15 (s, 9H). ¹³C{¹H} NMR (125 MHz, CDCl₃) δ : 170.4, 165.0, 162.9, 149.7, 149.4, 141.1, 129.1, 126.2, 114.1, 109.6, 109.4, 55.5, 51.8, 31.4, 29.8. HRMS (ESI-TOF) *m/z*: [M]⁺ calcd for [C₁₉H₂₃N₃O₃Na]⁺, 364.1637; found 364.1635.

4-(Dimethylamino)-N-(6-(3,3-dimethylbutanamido)pyridin-2-yl)benzamide (2g). **1c** (48 mg, 0.13 mmol) was placed in a vial in a glovebox. A solution of *bis*(pinacolato)diboron (36 mg, 0.14 mmol) in CH₃CN (10 mL) was then added to **1c** and allowed to stir for 24 h. The solvent was then removed, and the residue purified using column chromatography (SiO₂, 3:1 EtOAc/hexanes) to afford a white, chalky solid (40 mg, 87%). Mp = 207–209 °C. ¹H NMR (500 MHz, CDCl₃) δ : 8.23 (s, 1H), 8.09 (d, *J* = 8.5, 1H), 7.94 (d, *J* = 7.5, 1H), 7.82 (d, *J* = 8.5, 2H), 7.75 (t, *J* = 8.0, 1H), 7.66 (s, 1H), 6.72 (d, *J* = 9.0, 2H), 3.07 (s, 6H), 2.27 (s, 2H), 1.13 (s, 9H). ¹³C{¹H} NMR (125 MHz, CDCl₃) δ : 170.3, 165.3, 152.9, 150.2, 149.4, 140.8, 128.9, 120.4, 111.1, 109.6, 109.0, 51.8, 40.1, 31.4, 29.8. HRMS (ESI-TOF) *m/z*: [M]⁺ calcd for [C₂₀H₂₆N₄O₂Na]⁺, 377.1953; found 377.1966.

■ ASSOCIATED CONTENT

📄 Supporting Information

NMR spectra of new compounds, titration data, optimized geometries. This material is available free of charge via the Internet at <http://pubs.acs.org>.

■ AUTHOR INFORMATION

✉ Corresponding Author

*E-mail: pluth@uoregon.edu.

Notes

The authors declare no competing financial interest.

■ ACKNOWLEDGMENTS

This work was supported by funding from the University of Oregon. The NMR facilities at the UO are supported by the NSF/ARRA (CHE-0923589), and the computational infrastructure is supported by the OCI (OCI-096054). The Biomolecular Mass Spectrometry Core of the Environmental Health Sciences Core Center at Oregon State University is supported, in part, by the NIEHS (P30ES000210) and the NIH.

■ REFERENCES

- (1) Izatt, R. M.; Pawlak, K.; Bradshaw, J. S.; Bruening, R. L. *Chem. Rev.* **1995**, *95*, 2529–2586.
- (2) Evans, N. H.; Beer, P. D. *Angew. Chem., Int. Ed.* **2014**, *44*, 11716–11754.
- (3) Weisman, G. A.; Camden, J. M.; Peterson, T. S.; Ajit, D.; Woods, L. T.; Erb, L. *Mol. Neurobiol.* **2012**, *46*, 96–113.
- (4) Cetina, M.; Rissanen, K. *Croat. Chem. Acta.* **2012**, *85*, 319–325.
- (5) Schneider, H. J.; Yatsimirsky, A. K. *Chem. Soc. Rev.* **2008**, *37*, 263–277.
- (6) Therrien, B.; Vieille-Petit, L.; Tschan, M.; Romakh, V. B.; Suss-Fink, G. *Chimia* **2003**, *57*, 593–596.
- (7) Schneider, H. J. *Angew. Chem., Int. Ed.* **2009**, *48*, 3924–3977.
- (8) Reek, J. N. H.; Priem, A. H.; Engelkamp, H.; Rowan, A. E.; Elemans, J. A. A. W.; Nolte, R. J. M. *J. Am. Chem. Soc.* **1997**, *119*, 9956–9964.
- (9) McGrath, J. M.; Pluth, M. D. *J. Org. Chem.* **2014**, *79*, 711–719.
- (10) Chang, S. Y.; Kim, H. S.; Chang, K. J.; Jeong, K. S. *Org. Lett.* **2004**, *6*, 181–184.
- (11) Legrand, Y. M.; Gray, M.; Cooke, G.; Rotello, V. M. *J. Am. Chem. Soc.* **2003**, *125*, 15789–15795.
- (12) Londregan, A. T.; Storer, G.; Wooten, C.; Yang, X. J.; Warmus, J. *Tetrahedron Lett.* **2009**, *50*, 1986–1988.

(13) Kokatla, H. P.; Thomson, P. F.; Bae, S.; Doddi, V. R.; Lakshman, M. K. *J. Org. Chem.* **2011**, *76*, 7842–7848.

(14) Bordwell, F. G.; Mccallum, R. J.; Olmstead, W. N. *J. Org. Chem.* **1984**, *49*, 1424–1427.

(15) Hansch, C.; Leo, A.; Taft, R. W. *Chem. Rev.* **1991**, *91*, 165–195.

(16) Pellizzaro, M. L.; Fisher, J.; Wilson, A. J. *Rsc. Adv.* **2013**, *3*, 3103–3108.

(17) Gooch, A.; McGhee, A. M.; Pellizzaro, M. L.; Lindsay, C. I.; Wilson, A. J. *Org. Lett.* **2011**, *13*, 240–243.

(18) The binding constants do not trend with the σ^+ or σ^- Hammett parameters indicating that the effect of the electronic group is due to inductive rather than resonance effects. Additionally, the ^1H NMR chemical shifts of the phenyl hydrogens do not shift during the titrations, suggesting that there are no significant changes in resonance structures upon barbiturate binding.

(19) Ul Hoque, M. E.; Guha, A. K.; Kim, C. K.; Lee, B. S.; Lee, H. W. *Org. Biomol. Chem.* **2009**, *7*, 2919–2925.

(20) Creary, X.; O'Donnell, B. D.; Vervaeke, M. *J. Org. Chem.* **2007**, *72*, 3360–3368.

(21) Um, I. H.; Chung, E. K.; Kwon, D. S. *Tetrahedron Lett.* **1997**, *38*, 4787–4790.

(22) Chae, M. K.; Cha, G. Y.; Jeong, K. S. *Tetrahedron Lett.* **2006**, *47*, 8217–8220.

(23) Leventis, N.; Rawaswdeh, A. M. M.; Zhang, G. H.; Elder, I. A.; Sotiriou-Leventis, C. *J. Org. Chem.* **2002**, *67*, 7501–7510.

(24) Li, Y. L.; Flood, A. H. *J. Am. Chem. Soc.* **2008**, *130*, 12111–12122.

(25) Wilcox, C. S.; Kim, E.; Romano, D.; Kuo, L. H.; Burt, A. L.; Curran, D. P. *Tetrahedron* **1995**, *51*, 621–634.

(26) Thordarson, P. *Chem. Soc. Rev.* **2011**, *40*, 1305–1323.

(27) Frisch, M. J.; Trucks, G. W.; Schlegel, H. B.; Scuseria, G. E.; Robb, M. A.; Cheeseman, J. R.; Scalmani, G.; Barone, V.; Mennucci, B.; Petersson, G. A.; Nakatsuji, H.; Caricato, M.; Li, X.; Hratchian, H. P.; Izmaylov, A. F.; Bloino, J.; Zheng, G.; Sonnenberg, J. L.; Hada, M.; Ehara, M.; Toyota, K.; Fukuda, R.; Hasegawa, J.; Ishida, M.; Nakajima, T.; Honda, Y.; Kitao, O.; Nakai, H.; Vreven, T.; Montgomery, J. A., Jr.; Peralta, J. E.; Ogliaro, F.; Bearpark, M.; Heyd, J. J.; Brothers, E.; Kudin, K. N.; Staroverov, V. N.; Kobayashi, R.; Normand, J.; Raghavachari, K.; Rendell, A.; Burant, J. C.; Iyengar, S. S.; Tomasi, J.; Cossi, M.; Rega, N.; Millam, J. M.; Klene, M.; Knox, J. E.; Cross, J. B.; Bakken, V.; Adamo, C.; Jaramillo, J.; Gomperts, R.; Stratmann, R. E.; Yazyev, O.; Austin, A. J.; Cammi, R.; Pomelli, C.; Ochterski, J. W.; Martin, R. L.; Morokuma, K.; Zakrzewski, V. G.; Voth, G. A.; Salvador, P.; Dannenberg, J. J.; Dapprich, S.; Daniels, A. D.; Farkas, Ö.; Foresman, J. B.; Ortiz, J. V.; Cioslowski, J.; Fox, D. J. *Gaussian 09*; Gaussian, Inc.; Wallingford, CT, 2009.

(28) , V., Dennington, R.; Keith, T.; Millam, J. *GaussView*; Semichem Inc.: Shawnee Mission, KS, 2009.